Negative refraction of surface acoustic waves in the subgigahertz range

B. Bonello,[1,*] L. Belliard,[1] J. Pierre,[1] J. O. Vasseur,[2] B. Perrin,[1] and O. Boyko[1]
[1]*Institut des NanoSciences de Paris (INSP), UMR CNRS 7588, Université Pierre et Marie Curie, 140 rue de Lourmel, 75015 Paris, France*
[2]*Institut d'Electronique, Micro-électronique et de Nanotechnologie (IEMN), UMR CNRS 8520, Cité Scientifique, 59652 Villeneuve d'Ascq Cedex, France*
(Received 22 February 2010; revised manuscript received 30 June 2010; published 15 September 2010)

We used the picosecond ultrasonic technique to experimentally demonstrate the negative refraction of surface acoustic waves in a two-dimensional phononic crystal. The sample is made of a square lattice of circular voids drilled at the surface of a thick silica substrate. The lattice parameter is of a few micrometers. Broad band surface acoustic waves with Fourier components in the gigahertz range were excited. The negative refraction is observed for Rayleigh waves with frequencies in the second band and propagating along the direction ΓM in the reduced Brillouin zone. We then used a plane-wave expansion method to calculate the dispersion of the waves in our sample and to analyze our experimental data.

DOI: 10.1103/PhysRevB.82.104109 PACS number(s): 63.22.−m, 68.35.Iv, 63.20.D−

I. INTRODUCTION

The negative refraction of electromagnetic waves was first predicted in the late 1960s by Veselago[1] who analyzed theoretically the behavior of a virtual medium which permittivity ε and permeability μ are simultaneously negative. It was shown that such a "double-negative" optical material (also called "left-handed" material) is potentially interesting to create perfect optical lenses suitable to overcome the diffraction limit and to focus into a perfect image, all the Fourier components issued from a two-dimensional (2D) object.[2] More recently, Notomi[3] has pointed out that the effective index of photonic crystals can also be controlled through the band structure and that negative refraction can be observed in these artificial materials as well. In that case the negative refraction is the direct consequence of the bands folding and of the negative slope of some optical branches.

Similar approaches can be adopted with any classical waves, including acoustic waves.[4–7] Indeed, it is expected that the negative refraction of ultrasounds can be observed either in elastic metamaterials or in phononic crystals (PCs). The former are constituted by a set of local resonators embedded into a matrix; the dimensions of these resonators must be much less than the acoustic wavelength in the host media, so that both negative specific mass and negative bulk modulus can be defined through homogenization theories. However, for this condition to be fulfilled, the local resonators must be coupled to the matrix through a medium with very specific physical property, making these artificial structures hard to elaborate. In analogy with the photonic crystals, which are their optical counterparts, negative refraction can also occur in PCs and actually experimental evidences of this phenomenon were given by several groups. For instance, Ke *et al.*[8] have investigated the propagation of bulk acoustic waves through an array of metallic cylinders arranged with the triangular symmetry and immersed in water. They have demonstrated negative refraction for acoustic modes in the second band. Focusing of liquid surface waves by rigid cylinders assembled in a square lattice has also been observed.[9] More recently, Sukhovitch *et al.*[10] studied the refraction of bulk longitudinal waves caused by a 2D PC immersed in water and the focusing through a flat ultrasonic lens with a resolution just above the diffraction limit was realized.

However, in most of the studies performed to date, the matrix of the PC was a liquid, i.e., a medium where only longitudinal waves at moderate frequency can propagate. Actually, despite their interest for potential applications, the negative refraction of surface acoustic waves (SAWs) on PCs in solid matrix remains an uninvestigated topic to date. In this work, we were interested in the refraction of Rayleigh waves at several hundred of megahertz, propagating in a PC constituted by a 2D array of air inclusions drilled into a silica substrate. The lattice parameter of our sample being in the micrometer range, the experiments were conducted using the picosecond ultrasonic technique,[11,12] which is very well suited to measurements requiring ultimate spatial and temporal resolutions. We used this technique, initially developed for probing bulk longitudinal waves, to image the displacements field of surface waves on the output of the PC, after they have been refracted, in a large area straddling the normal to the interface. We have then calculated the band structure of our sample and we show in the following that surface modes in the second band are negatively refracted.

II. EXPERIMENTAL DETAILS

A square lattice of circular air inclusions has been drilled at the surface of a 2-mm-thick silica substrate by photolithography techniques and subsequent wet chemical etching. The large sample thickness, as compared to both the acoustic wavelength and the periodicity of the air inclusions, prevents from any reflection at the rear free surface of sample. We have therefore considered the substrate as semi-infinite in the direction normal to the lattice. The lattice parameter was $a=4$ μm and the filling fraction was slightly less than the close packing ($f=\pi/4$) so that the holes were not connected each others. The holes were ~ 1.3 μm deep and the overall shape of the PC was a triangular prism with 45° angles (Fig. 1). The sample was covered with a 50-nm-thick aluminum film, acting as a thermoelastic source under illumination by

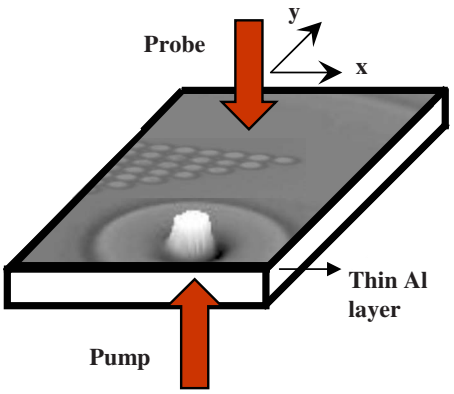

FIG. 1. (Color online) Schematic illustration of the experiment. A delay line (Newport model MM4006) allows for a maximum delay of 12 ns between the probe and the pump beams. The probe is focalized by an objective (NA=0.95) attached to a piezoelectric stage (Physik Instrumente model P-563.3CL) allowing for 100 $\times 100$ μm^2 scanning on the (x,y) plane.

an ultrashort light pulse and allowing for easier detection of the excited elastic waves. The elastic impedance of aluminum being almost equal to that of silica, this thin film did not affect the propagation of the Rayleigh waves.

We carried out the experiments using a picosecond ultrasonic setup. Up to now, this "pump and probe" technique has been used mainly to generate and to detect bulk elastic waves, longitudinal or transverse[13–15] as well, at frequency up to ~1 THz, allowing the investigation of the elastic properties of various systems, including thin films,[11] superlattices,[16,17] or isolated dots.[18] The generation and the detection of Rayleigh waves have been considered more recently.[19] Actually, the tremendous resolution in both space and time domains makes now possible to determine the acoustic dispersion of surface waves.[20] Moreover, the spectral content of the excited acoustic pulse can be controlled by tuning the focus of the pump pulse and surface acoustic waves with Fourier components in the gigahertz range are now routinely achieved. This feature is particularly relevant for studies dealing with phononic crystals since the phenomena expected in these systems are strongly frequency dependent.

In the present case, the surface elastic waves were excited from the back side of the sample, by illuminating the interface SiO_2/Al, through the SiO_2 substrate, with ultrashort optical pulses issued from a Ti:sapphire laser source (duration =100 fs, λ=800 nm). The probe beam, issued from the same laser source as the pump, was focused on the front side of the sample by an objective attached to a piezoelectric stage. It allowed to monitor the surface displacements at regularly spaced locations around the pump epicenter. Since the surface displacements only affect the imaginary part of the optical refractive index of aluminum, conventional measurements of the reflectivity changes were not appropriate in our case. Instead, in most of our experiments we used a stabilized Michelson interferometer to record images of the surface displacements at different time delays covering about 12.6 ns, i.e., the time interval between two consecutive excitation pulses. It is to be noticed that this interferometric method is only sensitive to the normal component of the displacements but not to the in-plane components. However, stabilizing the interferometer in the structured part of the sample is hard to achieve. This is the reason why we rather used a reflectivity scheme for measurements inside the PC itself and its immediate vicinity. Note also that the roughness of the sample was much less than any acoustic wavelength involved in the experiments and it did not affect the S/N ratio. Further details on both our reflection and transmission geometries are given elsewhere.[21,22]

III. RESULTS AND DISCUSSION

In a first set of experiments, we have focused the pump beam over a spot of ~3.5 μm, less than the lattice parameter of the sample. That insures that SAWs with **k** vectors extending beyond the first Brillouin zone are actually excited and undergo folding effects. We show in the lower part of Fig. 2(a) a typical reflectivity image for a 100×50 μm^2 region around the PC, recorded a few picoseconds after a light pulse has impacted the surface. The bright spot corresponds to the photothermal signature of the pump excitation. Note that the diameter is much larger than the laser focus itself, due to the thermal diffusion into the system. The holes lattice is clearly visible in the left-hand side of Fig. 2(a), owing to the reflectivity variations measured at the edges of the air inclusions.

The upper part of the figure represents a snapshot of the surface displacements measured in an interferometric scheme. The most striking feature in this figure is the highly contrasted ring that corresponds to the SAW which has emerged from the pump epicenter about 21.5 ns earlier. The grayscale in Fig. 2 stretching from negative values (deep) to positive values (bump) of the out-of-plane motion, one sees that the front wave has a dipolar shape, as expected for a Rayleigh wave excited in the thermoelastic regime. Let us compare the portion of the wave that has interacted with the PC (left-hand side of the dashed line) to the portion that has not (right-hand side). The broadening of the former suggests a poorer spectral content in comparison to the one of the latter which has not been altered through dispersion or diffusion processes during propagation.

This is further demonstrated in Fig. 3 where we compare the normal displacements as a function of time, in two different locations within the unpatterned region of the sample on either side of the dashed line drawn in Fig. 2 (dots 1 and 2), and their corresponding temporal Fourier transform. No noticeable alterations are detected for frequencies less than about 200 MHz, as expected for Rayleigh waves with wavelengths much larger than both the period and the depth of the air inclusions (the wavelength in silica at 200 MHz is ~16 μm). In contrast, high-frequency SAW components are strongly affected by the interaction with the PC and a significant damping is observed. This can be partly explained by partial reflections of the elastic waves when impinging the holes lattice but also, as discussed below, by the negative refraction of the waves, induced by the periodic patterning.

Behind the Rayleigh wave in Fig. 2(a), wavelets are also clearly visible on both sides of the normal to the outgoing

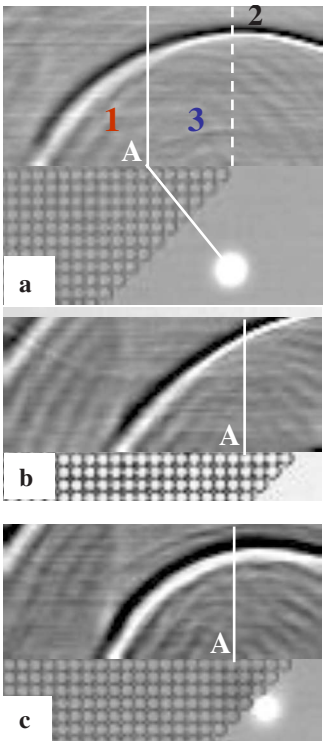

FIG. 2. (Color online) Horizontal scale is fixed at 100 μm for all snapshots. The upper part of each picture corresponds to SAW mapping using an interferometric scheme. The full line issued from point A is the normal to the PC/uniform medium interface. The dashed line marks the limits of the interaction between the SAW and the PC. Lower part: because of the air hole, our actively stabilized interferometer cannot operate in this region of the sample. Instead we recorded the changes in reflectivity induced by the pump pulse on the Al transducer. Note that the two parts of the sample depicted in these snapshots perfectly match each other. Red (1) and blue (3) points show the places where the data displayed in Fig. 4 have been recorded. (a) Snapshot recorded at t=21.5 ns after the pump excitation. (b) Image recorded with the optical excitation at ~40 μm apart from the ingoing interface (out of the scanned area). (c) Image recorded when the laser excitation is located near the tip of the PC.

interface issuing from point A. Very similar results were obtained when the optical excitation was more distant from the PC, at about 40 μm apart from the ingoing interface [Fig. 2(b)]. In such experimental conditions, the Rayleigh wave exhibits a quasi planar wave front when impinging the outgoing interface. Consequently, all the experimental data may be interpreted taking only into account the direction [11] of the PC corresponding to propagation along ΓM in the reduced Brillouin zone. Then the point A is defined considering this relevant direction and the pump location.

From the temporal dependence of these acoustic wavelets recorded at positions marked by dots 1 and 3 in Fig. 2(a) and displayed in Fig. 4, we measured their frequencies to be centered on 400 MHz in the positive refraction zone and significantly larger, on 600 MHz, in the negative refraction zone, with spectral broadenings of 40 MHz and 60 MHz, respectively.

In Fig. 2(c), we show an image recorded with the pump excitation located in area near the tip of the PC. Again, high-

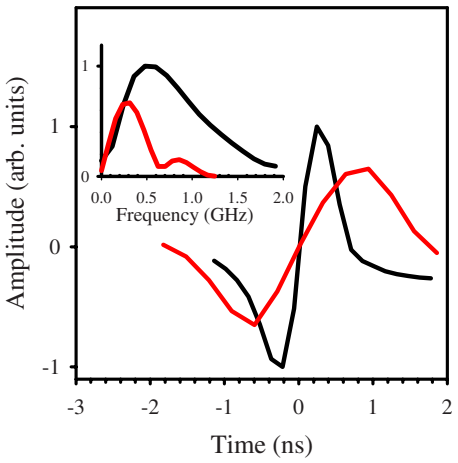

FIG. 3. (Color online) Out-of-plane displacements as a function of time recorded in the right-hand side (black) and in the left-hand side (red) of the dashed line in Fig. 2. Inset: corresponding temporal Fourier transforms.

frequency acoustic features are detected in the negative area. In such geometry the travel path within the PC is very short and thus the lack of high-frequency components in the left-hand side of the normal cannot be ascribed to damping processes.

Finally, it should also be noticed that both these wave packets propagating on either side of the outgoing normal have quasicircular wave fronts centered in point A. The deviation from pure circular wave fronts can be ascribed to the Fourier components of the wavelets which undergo different refraction angles.

To unambiguously establish that these vibrations actually propagate, we have imaged the surface of the sample at different times, with a delay of 1 ns between two consecutive frames (Fig. 5). The animation resulting from this set of

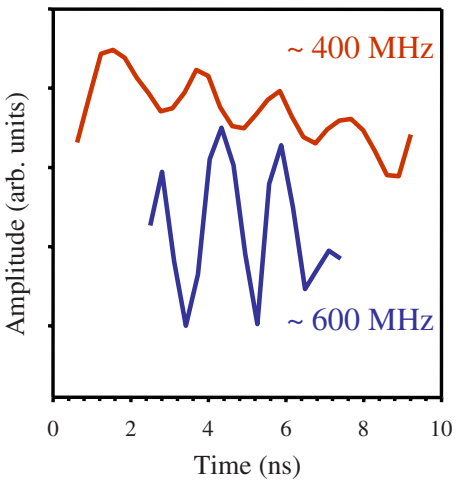

FIG. 4. (Color online) Out-of-plane displacements as a function of time recorded in the right-hand side of the full line (red—positive refraction) and in between the full line and the dashed line (blue—negative refraction) in Fig. 2. The time origin has been translated for clarity. Dots in Fig. 2 show the places where these data have been recorded.

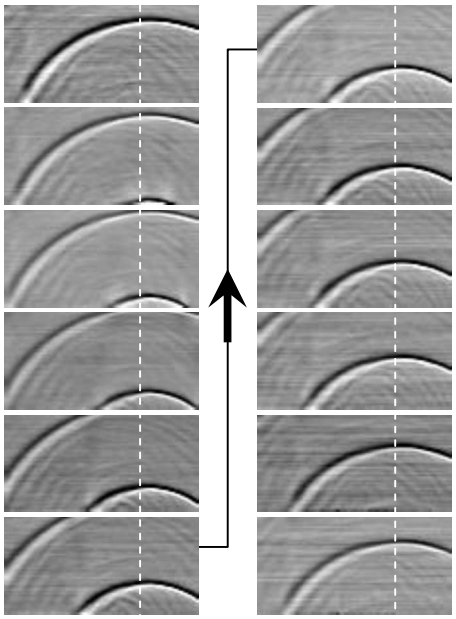

FIG. 5. Sequence of SAW images (100×50 μm^2) recorded every nanosecond during the laps of time separating two consecutive pump pulses (the repetition rate of our "Mai Tai" Spectra Physics laser is 80 MHz). The dash lines mark the tip of the triangular prism PC.

records[23] clearly shows that acoustic waves propagate in both sides of the normal to the interface, with a velocity of 3.2 nm ps^{-1}, equal to that of Rayleigh waves on the silica substrate. Moreover, from the refractive angles one could estimate the phase velocities of these modes in the CP to be about $v \approx 2.6$ nm ps^{-1} at 400 MHz and $v \approx 2.8$ nm ps^{-1} at 600 MHz.

In another set of experiments we have focused the pump beam over a spot of 10 μm in order to lower the maximum frequency of the excited surface waves down to about 450 MHz. The dispersion curves displayed below (see Fig. 7) shows that only SAWs with **k** vector along the first branch in ΓM were then excited into vibration. We have probed the same area of the sample as previously. The SAW image is shown in Fig. 6. No changes were induced by these new experimental conditions for the positively refracted waves and we measured the central frequency of the wavelets to be still ~400 MHz, within the experimental uncertainty. In contrast, no oscillations were detected in the region of negative refraction, i.e., in the right-hand side of the outgoing normal.

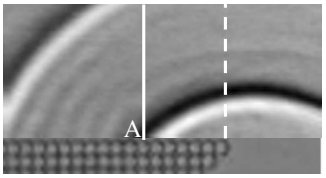

FIG. 6. SAW image recorded after the sample has been excited into vibrations by a laser pulse focalized within a ~10 μm spot in order to lower the maximum acoustic frequency down to ~450 MHz.

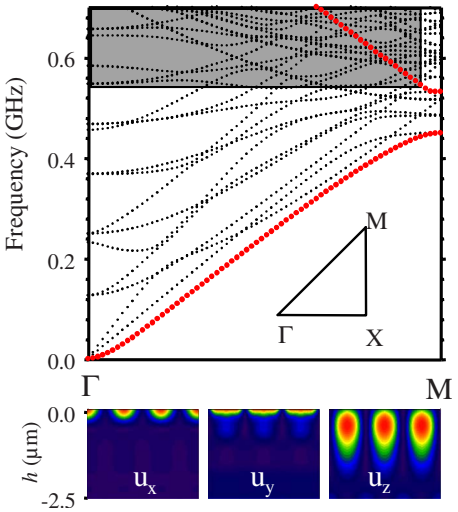

FIG. 7. (Color online) Band structure along ΓM. The red dots correspond to the Rayleigh waves identified by the displacements field shown in the bottom of the figure. The displayed displacements field is calculated for a frequency in the second band. The gray rectangle shows the frequency range where negative refraction is expected to occur.

Further insight into these results can be obtained from the examination of the band structure for the PC sample used in the experiments. One considers a silica plate of thickness $h = 1.3$ μm in which a square array of holes has been drilled deposited onto a homogeneous silica substrate of thickness d. We have computed the dispersion curves of this PC structure using the supercell (SC) plane-waves expansion method described elsewhere.[24] In our method, the PC structure is covered with a slab of thickness d' made of a fictitious low impedance material with very low density and very high speeds of sound modeling vacuum. This allows us to define a three-dimensional SC with height along the vertical axis of unit vector **z** is $l=h+d+d'$. This SC is then periodically repeated along the three spatial directions and the equations of propagation are Fourier transformed. Due to their very low impedance in comparison to that of the phononic slab, the fictitious material forbids the interaction between the vibrational modes of neighboring periodically repeated PC plates. The Rayleigh modes are obtained as the limit of Lamb modes in a PC structure as the thickness d of the substrate goes to infinity. In practice, one considers d much larger than h.

The result for any **k** vector along ΓM in the reduced Brillouin zone and for frequencies up to 700 MHz is displayed in Fig. 7, where the Rayleigh waves are shown as red dots. It is to be noticed that the computations involving necessary a finite value for the thickness d (here $d=3a=12$ μm), "ghost solutions" corresponding to elastic modes guided on the rear surface or in between the free surfaces, may appear in the dispersion curves. We have therefore computed the components of the displacement vector **u** to distinguish the Rayleigh waves among all solutions (see Fig. 7). As a consequence of the periodicity, band gaps and subsequent folding of the branches, open for the Rayleigh waves at points X and M in the reduced Brillouin zone. The central frequency and

the magnitude of these gaps are, respectively, 350 MHz, 25 MHz at point X (not shown here) and 490 MHz, 65 MHz at point M. Furthermore, we calculated the phase velocity of the Rayleigh waves along the direction ΓM in the PC to be $v=\omega/k=2.60$ nm ps^{-1} at 400 MHz and $v=2.90$ nm ps^{-1} at 600 MHz, in good agreement with the values deduced from the measured refractive angles (see above).

In fact, the folding of a dispersion branch is not a sufficient condition for the negative refraction to occur. In addition, the wave vector **k** and the group velocity $\mathbf{v_G}$ have to be antiparallel to each other.[10] This condition is fulfilled when the frequency increases for decreasing magnitudes of the wave vector **k**, as it is the case for the Rayleigh mode in the second branch.

In addition the waves impinging on the interface PC/substrate at point A in Fig. 2(a), have a **k** vector along ΓM, i.e., along [11] in the direct space. This direction being an axis of symmetry for the CP, then the group velocity vector and **k** vector are antiparallel to each other. Moreover, the conservation of the **k** component along the surface of refraction results in the negative refraction effect, if the negative slope curve is above the corresponding silicate line. Thus, negative refraction is expected to occur in the frequency range marked by a gray rectangle in Fig. 7, (i.e., above 530 MHz), in very good agreement with our experimental results.

IV. CONCLUSIONS

Negative refraction of Rayleigh waves at frequencies in the subgigahertz range, in a phononic crystal made of periodic air inclusions into a solid matrix, was achieved. By tuning the Fourier components of the excited waves, we have shown that the phenomenon occurs for frequencies in the second band of the dispersion curves, as predicted both by fundamental considerations and by numerical simulations. 2D mappings of the surface displacements recorded as time elapses, allowed the direct observation of the refractive properties of the sample, in good agreement with our dispersion curves simulations. Such an evidence of the negative refraction of surface acoustic waves phononic crystals with solid matrix open a virgin application field. Indeed, it is now conceivable to integrate such phononic crystals with specific focusing or filtering properties into microelectronic devices. Frequency domain up to few 10 GHz, only limited by the crystal patterning, might be achieved in a very next future. Taking advantage of the high temporal time resolution allowed by our picosecond ultrasonic approach, very low sample periodicity patterning, close to the photonic one's, may be investigated. By this way, further investigation on the sound and photon interaction in such artificial systems seems to be now possible.

ACKNOWLEDGMENTS

We thank A.-C. Hladky-Hennion for fruitful discussions. Financial support from Agence Nationale de la Recherche (Grant No. ANR-08-BLAN-0101-02) is gratefully acknowledged.

*bernard.bonello@insp.jussieu.fr

[1] V. G. Veselago, Sov. Phys. Usp. **10**, 509 (1968).
[2] J. B. Pendry, Phys. Rev. Lett. **85**, 3966 (2000).
[3] M. Notomi, Phys. Rev. B **62**, 10696 (2000).
[4] M. H. Lu, C. Zhang, L. Feng, J. Zhao, Y. F. Chen, Y. W. Mao, J. Zi, Y. Y. Zhu, S. N. Zhu, and N. B. Ming, Nature Mater. **6**, 744 (2007).
[5] L. Feng, X. P. Liu, M. H. Lu, Y. B. Chen, Y. F. Chen, Y. W. Mao, J. Zi, Y. Y. Zhu, S. N. Zhu, and N. B. Ming, Phys. Rev. Lett. **96**, 014301 (2006).
[6] S. Zhang, L. Yin, and N. Fang, Phys. Rev. Lett. **102**, 194301 (2009).
[7] L. Feng, X. P. Liu, Y. B. Chen, Z. P. Huang, Y. W. Mao, Y. F. Chen, J. Zi, and Y. Y. Zhu, Phys. Rev. B **72**, 033108 (2005).
[8] M. Ke, Z. Liu, C. Qiu, W. Wang, J. Shi, W. Wen, and P. Sheng, Phys. Rev. B **72**, 064306 (2005).
[9] X. Hu, Y. Shen, X. Liu, R. Fu, and J. Zi, Phys. Rev. E **69**, 030201(R) (2004).
[10] A. Sukhovich, L. Jing, and J. H. Page, Phys. Rev. B **77**, 014301 (2008).
[11] C. Thomsen, H. T. Grahn, H. J. Maris, and J. Tauc, Phys. Rev. B **34**, 4129 (1986).
[12] B. Bonello, B. Perrin, E. Romatet, and J.-C. Jeannet, Ultrasonics **35**, 223 (1997).
[13] D. H. Hurley, O. B. Wright, O. Matsuda, V. E. Gusev, and O. V. Kolosov, Ultrasonics **38**, 470 (2000).
[14] T. Pezeril, P. Ruello, S. Gougeon, N. Chigarev, D. Mounier, J.-M. Breteau, P. Picart, and V. E. Gusev, Phys. Rev. B **75**, 174307 (2007).
[15] T. Dehoux, N. Chigarev, C. Rossignol, and B. Audoin, Phys. Rev. B **77**, 214307 (2008).
[16] W. Chen, Y. Lu, H. J. Maris, and G. Xiao, Phys. Rev. B **50**, 14506 (1994).
[17] L. Belliard, A. Huynh, B. Perrin, A. Michel, G. Abadias, and C. Jaouen, Phys. Rev. B **80**, 155424 (2009).
[18] A. Vertikov, M. Kuball, A. V. Nurmikko, and H. J. Maris, Appl. Phys. Lett. **69**, 2465 (1996).
[19] B. Bonello, A. Ajinou, V. Richard, Ph. Djemia, and S. M. Cherif, J. Acoust. Soc. Am. **110**, 1943 (2001).
[20] Y. Sugawara, O. B. Wright, O. Matsuda, M. Takigahira, Y. Tanaka, S. Tamura, and V. E. Gusev, Phys. Rev. Lett. **88**, 185504 (2002).
[21] T. Bienville, J.-F. Robillard, L. Belliard, I. Roch-Jeune, A. Devos, and B. Perrin, Ultrasonics **44**, e1289 (2006).
[22] F. Decremps, L. Belliard, B. Perrin, and M. Gauthier, Phys. Rev. Lett. **100**, 035502 (2008).
[23] See supplementary material at http://link.aps.org/supplemental/10.1103/PhysRevB.82.104109 for an animation showing the propagation in the (x,y) plane.
[24] J. O. Vasseur, P. A. Deymier, B. Djafari-Rouhani, Y. Pennec, and A.-C. Hladky-Hennion, Phys. Rev. B **77**, 085415 (2008).